

Theory of off-center impurities in silicon: Substitutional nitrogen and oxygen

Gary G. DeLeo, W. Beall Fowler, and George D. Watkins

Department of Physics, Lehigh University, Bethlehem, Pennsylvania 18015

(Received 6 October 1983)

The single-particle electronic structures and atomic displacements of substitutional nitrogen and oxygen in silicon are treated theoretically in a cluster representation using both the scattered-wave $X\alpha$ (SW- $X\alpha$) and modified neglect of diatomic overlap (MNDO) electronic-structure methods. Substitutional carbon and sulfur are treated to a lesser degree for the purpose of comparison. The impurity X and its environment are simulated by the clusters XSi_4H_{12} (SW- $X\alpha$ and MNDO) and $XSi_{16}H_{36}$ (MNDO only). In all cases, we find a localized occupied a_1 state in the gap with a localized unoccupied t_2 state above it when the impurity atoms are on center. Using computed MNDO total energies for XSi_4H_{12} as a function of impurity displacement, we find spontaneous displacement directions correctly predicted for neutral carbon, nitrogen, oxygen, and sulfur, and for negative oxygen. By monitoring the single-particle energies and eigenvectors, we identify the driving force for the spontaneous asymmetric displacements as a pseudo-Jahn-Teller effect. We further explore the total energy with respect to simultaneous impurity and near-neighbor-silicon displacements, where the effect of the host outside the cluster is simulated by "external springs" connected to the four silicon atoms of the cluster. We find that it is necessary to use effective springs that are quite different from those which follow from a valence-force treatment in order to reproduce the observed spontaneous displacements of the substitutional nitrogen and oxygen impurities. This failure of the simple valence-force treatment is discussed. Our results also suggest a model for the "thermal donor" in silicon, whereby a substitutional oxygen is pushed "on center" by the strain field due to surrounding oxygen interstitials.

I. INTRODUCTION

A wide variety of substitutional impurities have been studied in silicon.¹ In many cases, the impurities are found to occupy the high-symmetry tetrahedral (T_d) site, thereby fourfold coordinating with the near neighbors just as a silicon atom would. In some cases, however, the impurity resides "off center" in a site of lower symmetry (C_{2v} , C_{3v} , . . .) with a reduced coordination number. Consider the substitutional impurities carbon, nitrogen, oxygen, and sulfur. Although their electronic structures as free atoms are rather similar, they behave very differently as substitutional impurities. Carbon^{2,3} and sulfur⁴ are known from experiment to reside at the high-symmetry (T_d) site, while nitrogen⁵ and oxygen^{6,7} displace spontaneously off center in different directions. Oxygen is observed to be a single acceptor,^{8,9} yet sulfur is a double donor.¹⁰ In the present investigation we treat the electronic structure and spontaneous displacement of this interesting sequence of impurities theoretically, with emphasis on the off-center impurities, nitrogen and oxygen. In addition, the role of spontaneous silicon-neighbor displacements is critically examined.

Spontaneous impurity displacements are well known for defects in the ionic materials where classical electrostatic^{11,12} and quantum-mechanical^{13,14} models have been proposed to explain them. The most widely studied defect of this type is substitutional Li^+ in KCl .^{14,15} In the purely covalent materials, on the other hand, one would not expect classical electrostatic arguments to be adequate; hence, chemical mechanisms (e.g., "rebonding") have been

proposed. The interesting feature of the covalent materials is the variety of impurity displacements which are exhibited by such similar impurity atoms located in identical environments.

The substitutional oxygen impurity in silicon, commonly called the "A center," was identified by Watkins and Corbett^{6,7} and has been well characterized by electrical measurements,^{8,9} infrared absorption,⁷ and electron paramagnetic resonance (EPR).^{6,16} These studies have revealed that the A center is an acceptor whose level position lies at $E_c - 0.17$ eV. The substitutional oxygen in both stable charge states (neutral and single negative) was determined to be off center in a $\langle 100 \rangle$ direction, thereby reducing the symmetry to C_{2v} . The barrier for reorientation between equivalent directions has been measured for the neutral species and found to be 0.38 eV. The paramagnetic species is O^- . Here, the unpaired electron was found to reside mainly (71%) on the two near-neighbor silicons which are opposite the oxygen displacement direction. From stress measurements, this orbital was identified as antibonding with respect to these two silicon atoms.

More recently, neutral substitutional nitrogen in silicon has been identified by Brower.⁵ As with nitrogen in diamond,¹⁷ it displaces off center, but along a $\langle 111 \rangle$ axis, thereby lowering its symmetry to C_{3v} . The barrier for reorientation between equivalent directions was measured and found to be ~ 0.11 eV. It is a deep donor, and the unpaired electron of the neutral impurity is localized mainly ($\sim 72\%$) on the single near-neighbor silicon along $\langle 111 \rangle$, and slightly ($\sim 9\%$) on the nitrogen (72% p , 28% s); it is antibonding between the two of them.

Theoretical studies of substitutional nitrogen and oxygen in tetrahedrally bonded covalent materials¹⁸⁻³⁰ began

with the treatment of nitrogen in diamond by Messmer and Watkins.¹⁸ Extended Hückel theory (EHT) was used to estimate the total energy and single-particle electronic structure of a finite-cluster representation of the host and impurity. The resulting single-particle electronic structure for the on-center (T_d) impurity predicted a partially occupied t_2 state in the "gap," and above it an unoccupied a_1 state. Recognizing the Jahn-Teller instability associated with the partially occupied orbitally degenerate state (t_2), Messmer and Watkins then included symmetry-lowering displacements involving the nitrogen and four near-neighbor carbon atoms, with the result that the total energy decreased and then stabilized in a $\langle 111 \rangle$ off-center trigonal displacement, consistent with experiment. Subsequent to the calculations of Messmer and Watkins, a number of theoretical treatments of nitrogen in diamond and silicon have appeared which support this a_1 - t_2 ordering (t_2 below a_1),²⁰⁻²⁴ and hence the presence of a Jahn-Teller instability.

A recent self-consistent Green's-function calculation for on-center nitrogen in diamond by Bachelet, Baraff, and Schlüter²⁵ revealed, however, a reversal of the a_1 - t_2 order. Here, the a_1 state is lower and, hence, occupied by one electron; the t_2 state is a resonance in the conduction band. A tight-binding Green's-function calculation of Hjalmanson *et al.*²⁶ gives a similar ordering for nitrogen in silicon (a_1 below t_2). Lannoo³⁰ argues that EHT would also give a_1 below t_2 provided that a more appropriate parametrization were used. Impurity displacement was not considered in these treatments.

Theoretical calculations of substitutional oxygen in silicon have been reported as well. EHT cluster treatments of the on-center impurity have been found to give a doubly occupied t_2 state below an unoccupied a_1 state.²³ A tight-binding Green's-function calculation of Hjalmanson *et al.*²⁶ gives a_1 below t_2 as does the scattered-wave $X\alpha$ (SW- $X\alpha$) treatment of Caldas, Leite, and Fazzio²⁷ which uses a Watson-sphere termination. This a_1 - t_2 ordering has been found by the recent self-consistent Green's-function calculations of Singh, Zunger, and Lindefelt,²⁸ and of Car and Pantelides.²⁹ In the former calculation, both states are conduction-band resonances.

It is clear, therefore, that the more recent calculations indicate that for on-center nitrogen in diamond and silicon, and for on-center oxygen in silicon, the single-particle a_1 state (occupied) is below the t_2 state (unoccupied). This of course raises the question as to why nitrogen and oxygen spontaneously displace off center, since the ground state is no longer degenerate. This is an issue of current controversy. In the present investigation, we further explore the single-particle electronic structures of substitutional carbon, nitrogen, oxygen, and sulfur with particular emphasis on nitrogen and oxygen.³¹ We then study the spontaneous impurity and near-neighbor displacements employing a method conventionally used in molecular-geometry studies. These methods are described in the following section.

II. METHODS

The impurity electronic structures which we describe below involve the following two classes of approxima-

tions. (i) We simulate the impurity environment by small fragments of crystalline silicon, suitably terminated by hydrogen atoms, i.e., we use a "cluster approach." (ii) The eigenstates appropriate to these clusters are approximated by two electronic-structure methods which will be seen to have complementary advantages.

In the SW- $X\alpha$ method,^{32,33} the atoms which form the cluster and the entire cluster itself are surrounded by nonoverlapping spheres, thereby partitioning space into three regions: atomic, interatomic, and extramolecular. The potential, with a Slater statistical exchange,³⁴ is spherically averaged in the atomic and extramolecular regions and volume averaged in the interatomic region. This is the muffin-tin approximation. The eigenvalues and wave functions are determined by the condition that the wave function and logarithmic derivatives be continuous at all sphere boundaries. This process of generating wave function, then potential, is iterated until self-consistency is achieved.

The modified neglect of diatomic overlap (MNDO) approach³⁵ is a semiempirical Hartree-Fock linear combination of atomic orbitals—molecular orbital method which has evolved from the complete neglect of differential overlap method.³⁶ In this approximation, all of the one-center and some of the two-center integrals are retained; the others are set equal to zero. The one-center integrals are determined by fitting to experimental atomic data. The nonvanishing two-center integrals are parametrized by fitting to available experimental small-molecule data such as dipole moments, heats of formation, and bond lengths. As in the SW- $X\alpha$ method, the computational sequence is carried to self-consistency. Open shells are handled by the half-electron approximation,³⁷ where the total-energy expression is adjusted to agree with the appropriate Roothan open-shell total-energy expression³⁸ after self-consistency has been achieved.

Both electronic-structure methods provide single-particle electronic structures. It is well known, however, that the relationship between single-particle energy differences ($\Delta\epsilon$) and the corresponding total-energy differences (ΔE) depends on the method considered. In the SW- $X\alpha$ method, the $\Delta\epsilon$'s and ΔE 's typically differ by ~ 0.1 eV,³⁹ so that the $\Delta\epsilon$'s provide reasonable transition energies (ΔE 's) at a glance. This is characteristic of local-density methods. For MNDO, on the other hand, which is a Hartree-Fock method, these can be quite different when relatively localized states are involved,⁴⁰ as they always are in a cluster representation. The SW- $X\alpha$ single-particle *electronic* structures therefore contain a greater amount of useful information.

Because of the muffin-tin approximation, the SW- $X\alpha$ method fails to provide meaningful total-energy changes with impurity displacement. The MNDO method, on the other hand, is designed to provide realistic molecular geometries and is therefore well suited for calculations of total energy versus displacement. The total energies can then be monitored as a function of impurity-atom and neighboring-atom displacements to determine equilibrium conformations.

Both methods, SW $X\alpha$ and MNDO, can provide single-particle electronic structures for a given impurity

system. Therefore, by applying both of these electronic-structures schemes to a given system we are provided with a measure of the severity of the collective approximations used in both methods. This global test is a valid one because the approximations involved are quite different between the two methods. In particular, one would not expect to find a similar ordering of states if these approximations were too extreme. Differences in the magnitudes of the relative energy separations between the two methods are expected, however, as a consequence of the different exchange formalisms used, that is, local density versus Hartree Fock.

We come now to the cluster representation of the impurity environment. We simulate the impurity X and its environment by two clusters, XSi_4H_{12} (denoted cluster SI4) and $XSi_{16}H_{36}$ (denoted cluster SI16), which are centered at the site of the missing silicon atom. The hydrogen atoms serve to terminate the cluster by tying up the silicon dangling bonds and simulating the missing, more distant, part of the solid.

For the SW- $X\alpha$ calculations, we consider only cluster SI4, with the impurity atom on center. Here, the Si-H distance is set equal to the Si-Si near-neighbor distance appropriate to crystalline silicon (2.35 Å). The exact distance one uses here is somewhat arbitrary; however, we have shown in previous publications³⁹ that making it larger than the natural Si-H bond length (1.48 Å) provides a simple way of producing a density of states near the band edges with which the defect states can interact.

For the MNDO calculations, we consider both clusters SI4 and SI16. We use an Si-H distance of 2.12 Å (90% of 2.35 Å) for SI4, representing an arbitrary compromise between the natural Si-H bond length and the crystalline-silicon Si-Si distance. In addition, we consider the effect of changing this distance in the range from 1.48 to 2.35 Å. The natural Si-H bond length (1.48 Å) is used for cluster SI16, since the near-band-edge states which couple to the defect states are provided partially by the Si-near-neighbor-to-Si-next-nearest-neighbor interactions which are present in this larger cluster.

Applying the MNDO method to both clusters, we first explore the total energies and single-particle states as a function of $\langle 100 \rangle$, $\langle 111 \rangle$, and $\langle \bar{1}\bar{1}\bar{1} \rangle$ impurity displacements, holding the other atoms of the cluster fixed. We later explore the total-energy surface as a function of combined impurity and near-neighbor silicon displacements.

III. COMPUTATIONAL RESULTS AND INTERPRETATIONS

A. On-center electronic structures

The single-particle electronic structures for our SI4 cluster representations of crystalline silicon⁴¹ and neutral on-center nitrogen and oxygen are shown in Figs. 1 and 2 using SW- $X\alpha$ and MNDO, respectively. The states $1t_1$ and $3a_1$ of Si_5H_{12} represent the "valence-band" and "conduction-band" edges, respectively, in our model system, with $1t_1$ being the last occupied state. When nitrogen or oxygen (or sulfur, not shown) replaces the central silicon, an a_1 ($3a_1$) state is pulled down into our model-

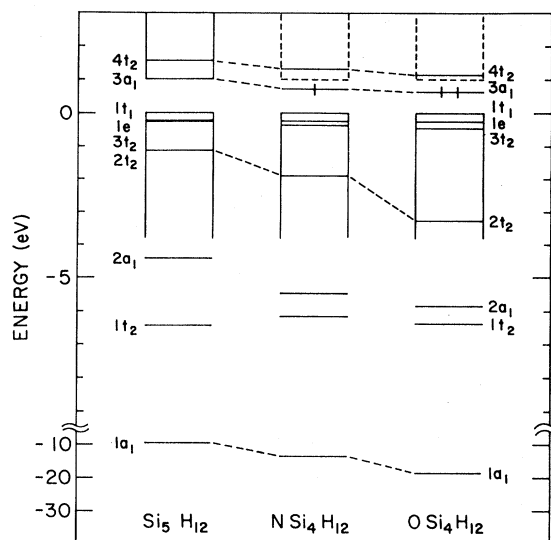


FIG. 1. Single-particle electronic structures for clusters Si_5H_{12} , NSi_4H_{12} , and OSi_4H_{12} ($d_{Si-H}=2.35$ Å) from SW- $X\alpha$. Valence-band maxima are set to zero.

system "band gap." This state and the $4t_2$ state above it are both somewhat localized on the central atom and the silicon ligands, but it is the lower-energy $3a_1$ state which is occupied by one electron for nitrogen and by two electrons for oxygen (and sulfur). Our computed $3a_1$ - $4t_2$ ordering is therefore consistent with the results of the more recent calculations on these and similar systems as

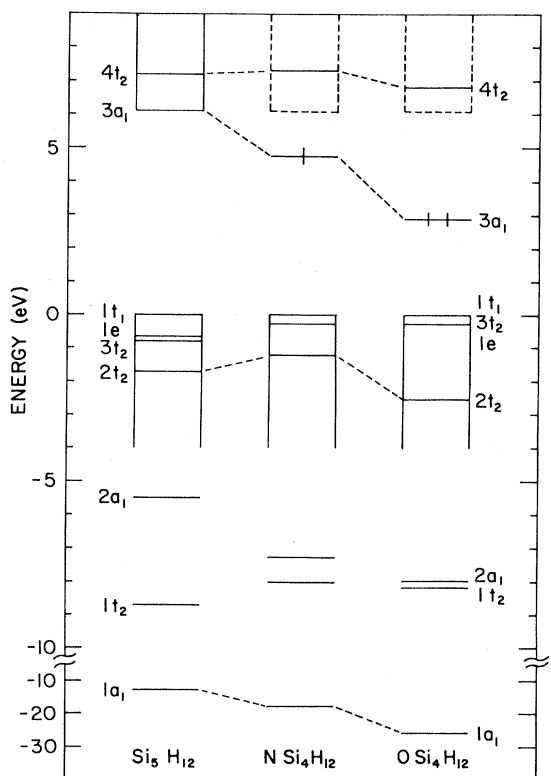


FIG. 2. Single-particle electronic structures for clusters Si_5H_{12} , NSi_4H_{12} , and OSi_4H_{12} ($d_{Si-H}=2.12$ Å) from MNDO. Valence-band maxima are set to zero.

described in the Introduction.

The $3a_1$ state is a deep level in the gap. The $4t_2$ state appears to be a conduction-band resonance. The $1a_1$ state which lies below the bottom of the valence band is mostly impurity s -like ($2s$ for N and O, $3s$ for S); the $2t_2$ state near the top of the valence band is mostly impurity p -like ($2p$ for N and O, $3p$ for S). These a_1 and t_2 states are the "hyperdeep" states described by Hjalmarson *et al.*²⁶

A simple argument presented by Bachelet, Baraff, and Schlüter²⁵ for why the a_1 state ought to be lower than the t_2 state is illustrated in Fig. 3. Here, the atomic valence s and p states are considered to interact with the a_1 and t_2 states of the lattice vacancy into which the impurity is inserted. This model clearly explains the presence of the gap (deep) and hyperdeep a_1 states as well as the resonant and hyperdeep t_2 states which we find.

A comparison of Figs. 1 and 2 reveals that there is a strong resemblance between the SW- $X\alpha$ and MNDO single-particle electronic structures. This similarity suggests that the SW- $X\alpha$ and MNDO approximations (muffin-tin and MNDO, respectively) are not too severe in these cases.

The differences present in single-particle energy spacings ($\Delta\epsilon$'s) between SW $X\alpha$ and MNDO are readily apparent, but most of these can be understood in terms of the relationship between these $\Delta\epsilon$'s and the excitation energies (ΔE 's) as described in the Introduction. A " Δ -SCF" calculation (where SCF denotes self consistent field) (ΔE 's) for the band gap of Si_3H_{12} using MNDO gives a ground-singlet ($1t_1^0$) to excited-singlet ($1t_1^5 3a_1^1$) energy separation of ~ 2 eV. Here, the ground- and excited-state energies are separately calculated self-consistently. This is much smaller than the single-particle energy separation between $1t_1$ and $3a_1$ of ~ 6 eV, and is much closer to the SW- $X\alpha$ excitation energy ($\Delta E \sim \Delta\epsilon$) of ~ 1 eV.

We now consider an approximation which is common to both of these calculations. In both SW $X\alpha$ and MNDO we have used the small SI4 clusters to simulate the impur-

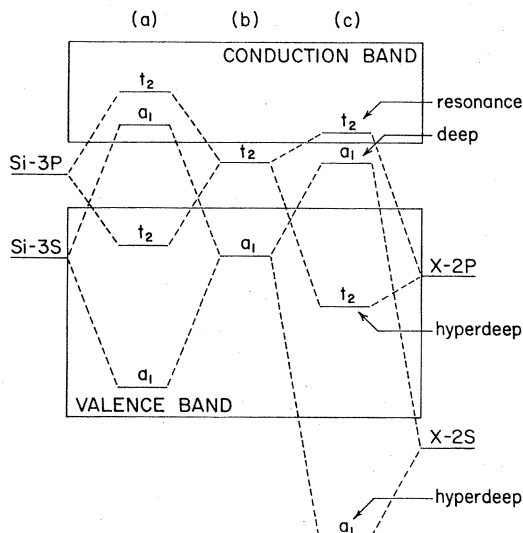


FIG. 3. Schematic representation of vacancy-impurity (and vacancy-silicon) interactions where (a) represents crystalline silicon, (b) the lattice vacancy, and (c) the substitutional impurity.

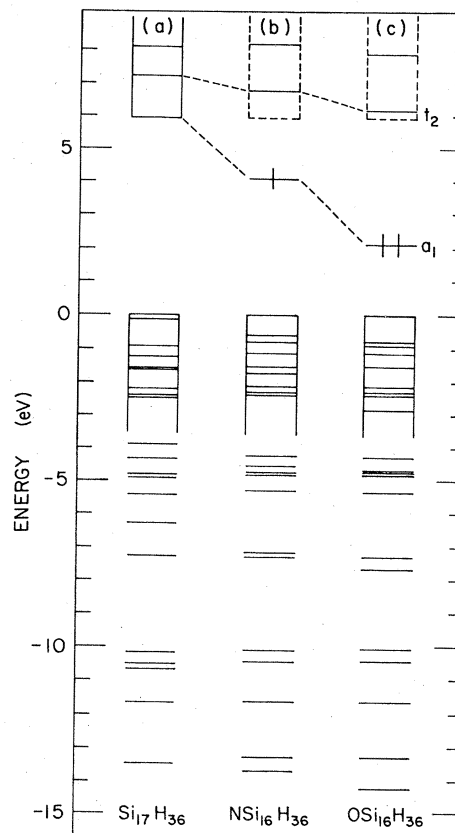


FIG. 4. Single-particle electronic structures for clusters $\text{Si}_{17}\text{H}_{36}$, $\text{NSi}_{16}\text{H}_{36}$, and $\text{OSi}_{16}\text{H}_{36}$ ($d_{\text{Si-H}} = 1.48$ Å) from MNDO. Valence-band maxima are set to zero. Note that the lowest a_1 state for each cluster is not shown in the figures. It would be located at -15.9 , -19.0 , and -26.6 eV for $\text{Si}_{17}\text{H}_{36}$, $\text{NSi}_{16}\text{H}_{36}$, and $\text{OSi}_{16}\text{H}_{36}$, respectively.

ity environment. In order to explore this approximation, we apply MNDO to these same impurity systems, but using the larger SI16 clusters. The corresponding SI16 single-particle electronic structures for crystalline silicon and on-center nitrogen and oxygen are shown in Fig. 4. In Fig. 5, the oxygen results from MNDO using SI16 [Fig. 5(a)] and SI4 [Fig. 5(b)] are shown together.

The single-particle electronic structures appropriate to the SI16 cluster are clearly similar to those from the smaller SI4 cluster. Although it is not shown, the same is true for sulfur. Here again we find a localized and occupied a_1 gap state directly below a localized and unoccupied t_2 resonant state. This suggests that the computed a_1 - t_2 ordering is not simply a small-cluster effect. In fact, there is very little change in the a_1 - and t_2 -state positions relative to each other and the valence-band maximum in going from SI4 to SI16. The choice of a larger than natural Si-H distance in SI4 is largely responsible for this good agreement, as demonstrated in Fig. 5(c) where we show the results for an SI4 cluster ($\text{OSi}_4\text{H}_{12}$), but with a natural Si-H distance of 1.48 Å (call this cluster SI4'). Here, the a_1 and t_2 states relative to the valence-band edge agree less well with those of cluster SI16.

A similar observation can be made by a comparison of

existing SW- $X\alpha$ calculations of substitutional oxygen. Caldas, Leite, and Fazzio²⁷ have used a Watson-sphere-terminated 16-silicon cluster, and they too find an a_1 state directly below an unoccupied t_2 state. Again, this demonstrates that this a_1 - t_2 ordering is not an anomalous small-cluster effect.

The computed single-particle electronic structures, therefore, would appear to predict that nitrogen is a single donor, and that oxygen and sulfur are double donors. However, contact with experiment cannot be made from these calculations for nitrogen and oxygen, since they are known from experiment to reside off center in a site of lower symmetry. Sulfur, on the other hand, is found from experiment to be on center and it is, in fact, a double donor. The first (single) donor level for sulfur is observed at $\sim E_c - 0.3$ eV,⁴² or relative to the valence band, $\sim E_v + 0.85$ eV. The SSi_4H_{12} SW- $X\alpha$ calculation of Carling⁴¹ which uses the type of cluster that we have called SI4, gives $\sim E_v + 0.9$ eV, as estimated from the $3a_1$ - $1t_1$ single-particle energy separation. This is in good agreement with experiment.

B. Defect geometries from MNDO

We now proceed to investigate symmetry-lowering displacements for substitutional nitrogen and oxygen using the MNDO method. Implicit in the following is the assumption that the processes which are important in determining molecular geometries are also those which are important here in determining impurity geometries. With this assumption, we can proceed in a very direct way to apply MNDO to the problems at hand.

The MNDO matrix elements have been determined elsewhere by fitting computational results to measured quantities from appropriate free atoms and small molecules.³⁵ Since few, if any, of these small molecules contain a Si-Si bond, it is not clear that such a bond would

be well represented using the reported silicon parametrization. We have therefore tested the Si-Si bond using the three clusters, $Si_{17}H_{36}$ (SI16), Si_5H_{12} (SI4'), and Si_8H_{18} , by allowing sets of silicon atoms to relax and seek out their equilibrium positions. The shell of four near-neighbor silicon atoms to the central silicon in $Si_{17}H_{36}$ remains essentially at 2.35 Å when allowed to move radially in a rigid cage. In the Si_5H_{12} cluster, the Si-Si distance for a SiH_3 unit moving rigidly relative to the rest stabilizes at ~ 2.25 Å. This same distance is found for the Si_2 bond length in Si_8H_{18} (H_9 - Si_3 - Si_2 - Si_3 - H_9) with one $Si-Si_3H_9$ unit moving rigidly against a similar unit where both use a natural Si-H distance of 1.48 Å. Therefore, we find that the Si-Si bond length of 2.35 Å is predicted in all cases to within < 0.1 Å. This is consistent with the MNDO results of Verwoerd⁴³ on silicon-containing molecules. Also, our computed Si-Si bond-stretching spring constant of ~ 11 eV/Å² (determined from Si_8H_{18} or $Si_{17}H_{36}$ as described above) is consistent with the value of ~ 10 eV/Å² determined from compressibility measurements.⁴⁴

In a more severe test, we have simulated the disiloxane molecule (OSi_2H_6), and we find that the Si-O and Si-H bond lengths are also properly reproduced. However, the Si-O-Si bond angle is predicted to be 180°, which is not consistent with the measured value of $\sim 144^\circ$. Large-basis-set *ab initio* Hartree-Fock calculations also predict this angle to be 180°. It has been argued that d functions are required in order to obtain agreement with experiment.⁴⁵ Fortunately, the Si-O-Si bond-bending energy is small and is, therefore, not a critical factor in determining the oxygen displacement in a cage of silicon atoms. Here, the important factor is the Si-O bond-stretching energy, which is well represented by this method.

C. Spontaneous impurity displacement in a rigid cage

We now apply the MNDO method to neutral substitutional nitrogen and oxygen in the SI4 cluster representation. The cluster total energies as functions of impurity displacements are shown in Figs. 6 and 7. Here, the other atoms are held fixed with the near-neighbor silicon atoms located at crystalline silicon sites. The nitrogen impurity is seen to be stable off center in a $\langle \bar{1}\bar{1}\bar{1} \rangle$ direction, thereby lowering its symmetry to C_{3v} . The oxygen impurity is stable off center in a $\langle 100 \rangle$ direction, thereby lowering its symmetry to C_{2v} . Not shown are neutral carbon and sulfur which are found to remain on center, and negative oxygen which also goes off center in a $\langle 100 \rangle$ direction. This simple model therefore predicts correctly the displacement directions for all five of these observed substitutional impurity systems.

Although we hesitate to take too seriously the details of these potential-energy curves in view of the simplicity of our model, we point out a few interesting features. The nitrogen exhibits a shallow on-center minimum and a deeper off-center minimum located at 0.55 Å in the $\langle \bar{1}\bar{1}\bar{1} \rangle$ direction with a depth of 0.05 eV. The barrier for reorientation is therefore ~ 0.05 eV; i.e., reorientation appears to require that the nitrogen go through or near the

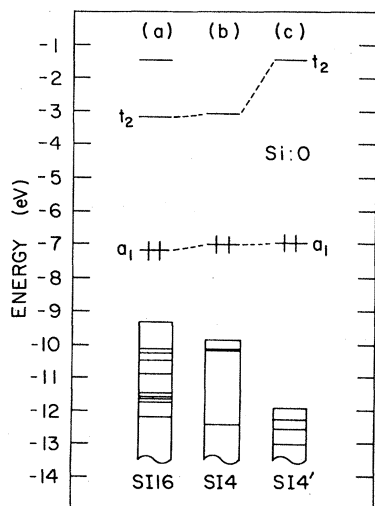


FIG. 5. Comparison of single-particle electronic structures for three cluster representations of substitutional oxygen: (a) $OSi_{16}H_{36}$ ($d_{Si-H} = 1.48$ Å), (b) OSi_4H_{12} ($d_{Si-H} = 2.12$ Å), and (c) OSi_4H_{12} ($d_{Si-H} = 1.48$ Å).

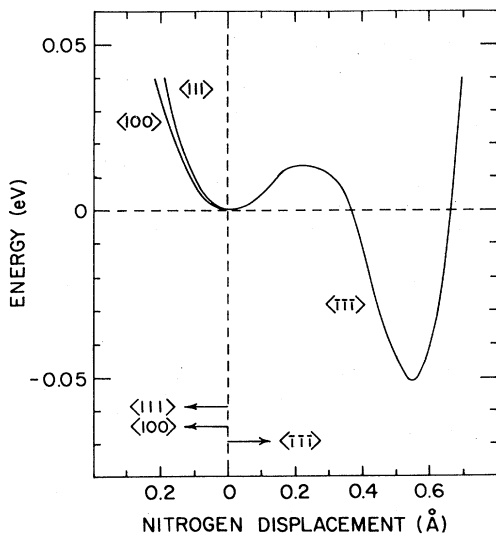


FIG. 6. Total energy of cluster $\text{NSi}_4\text{H}_{12}$ ($d_{\text{Si-H}}=2.12$ Å) from MNDO as a function of nitrogen displacement, where all other atoms are fixed.

origin since the $\langle 100 \rangle$ and $\langle 111 \rangle$ directions have no off-center minima. This energy is close to the observed barrier of 0.11 eV.⁵ The oxygen minimum is at 1.0 Å in the $\langle 100 \rangle$ direction with a depth of 1.0 eV. The corresponding reorientation barrier, estimated from the $\langle 110 \rangle$ minimum (the saddle point through which reorientation

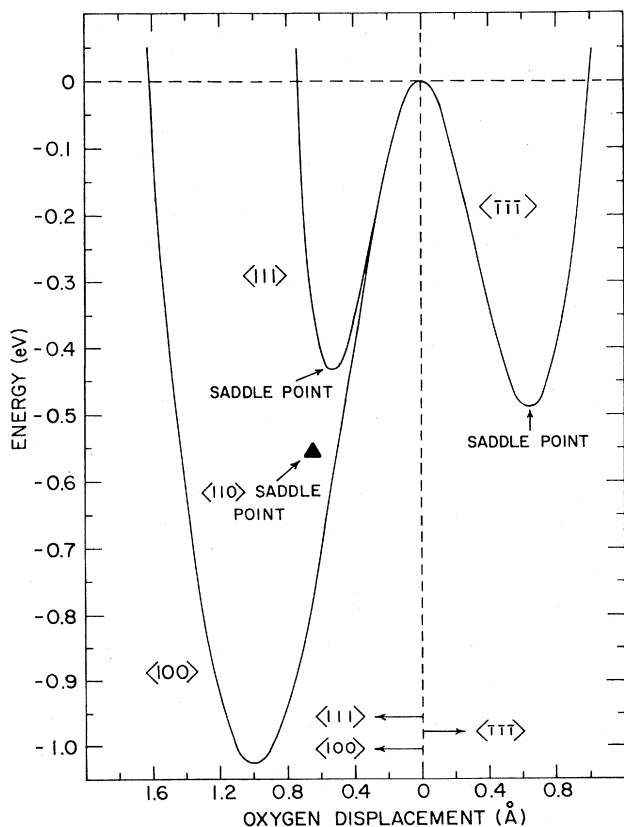


FIG. 7. Total energy of cluster $\text{OSi}_4\text{H}_{12}$ ($d_{\text{Si-H}}=2.12$ Å) from MNDO as a function of oxygen displacement, where all other atoms are fixed. The $\langle 110 \rangle$ saddle point (minimum along the $\langle 110 \rangle$ direction) is shown in the figure by a solid triangle.

occurs), is ~ 0.47 eV, again close to the observed barrier of 0.38 eV.⁶

Since the observed nitrogen and oxygen displacements are correctly predicted in this simple model, we proceed to use these single-particle results to develop an understanding of the driving force for this off-center behavior. We first consider the substitutional nitrogen single-particle electronic structure with respect to nitrogen $\langle \bar{1}\bar{1}\bar{1} \rangle$ displacement using the SI4 cluster representation. In Fig. 8(a) we show the energy eigenvalues corresponding to the states $3a_1$ and $4t_2$ (call them a_1 and t_2). The t_2 state couples to the trigonal displacement and, hence, splits into states of a_1 (labeled a_1'') and e symmetry in C_{3v} . (Correspondingly, we label as a_1' the state deriving from the $3a_1$ state in T_d symmetry.) The curvature in the a_1' state and an accompanying lowering of the a_1' state suggest coupling between the two states produced by the displacement.¹³ Such a coupling, if large enough, could provide the driving force for the displacement.

In the single-particle picture, the Hamiltonian matrix for linear Jahn-Teller electron-lattice coupling within these two states can be written in terms of the a_1 (a_1') and $t_2\langle 111 \rangle$ (a_1'') basis states as^{13,30}

$$\begin{bmatrix} \Delta - IQ & GQ \\ GQ & 0 \end{bmatrix}$$

Here, Δ is the t_2 - a_1 separation, Q the trigonal (t_2) displacement coordinate, I the trigonal Jahn-Teller coupling coefficient for the excited t_2 state, and G the coupling coefficient which provides off-diagonal a_1 - $t_2\langle 111 \rangle$ coupling.

As discussed recently by Lannoo³⁰ in a total-energy

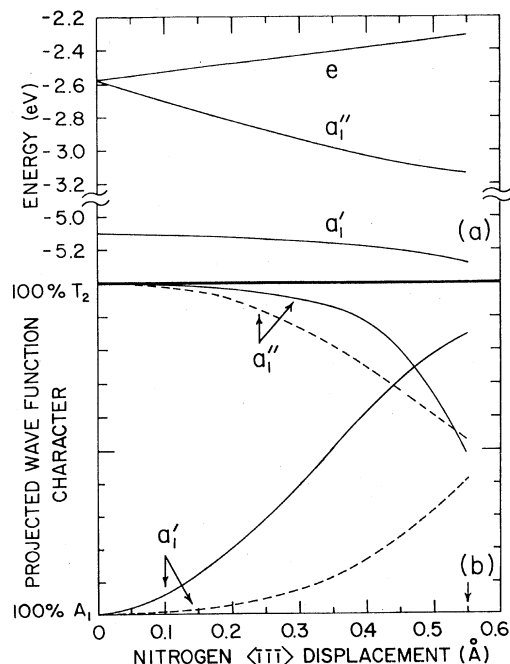


FIG. 8. (a) Energies of $3a_1$ (a_1') and $4t_2$ (a_1'' , e) states vs nitrogen $\langle \bar{1}\bar{1}\bar{1} \rangle$ displacement for $\text{NSi}_4\text{H}_{12}$ ($d_{\text{Si-H}}=2.12$ Å) from MNDO. (b) Projected A_1 and T_2 (in T_d) character on nitrogen (solid line) and on ligands (dashed line). The arrow on the displacement axis denotes the position of minimum total energy.

framework (including the elastic energy, $\frac{1}{2} kQ^2$) for the similar problem of nitrogen in diamond, this can provide a stable off-center trigonal displacement for the lower-energy state for a continuous range of values for G and I between the two extremes: (i) $G=0$, $I^2/k > 2\Delta$, and (ii) $I=0$, $G^2/k > \Delta/2$. The first can be considered a pure Jahn-Teller splitting of the excited t_2 state which provides a lower off-center minimum energy than the "ground" a_1 undisplaced state. The second case is a pure "pseudo-Jahn-Teller" effect, where the interaction is purely off diagonal between the two a_1 states.

It is difficult to decide from the eigenvalues of Fig. 8(a) which of these extremes better describes our situation, or if it is something in between. The reason for this is that the separation between the occupied and unoccupied states is exaggerated, as described earlier. We therefore look instead at the eigenvectors, that is, the character of the wave functions as a function of displacement.

We project out of the a_1' and a_1'' states the a_1 and t_2 components (in T_d) as a function of displacement. This is shown in Fig. 8(b) separately for the contribution on the central nitrogen atom and on the four silicon neighbors. On the nitrogen atom, the a_1 and t_2 components are simply the fractional $2s$ and $2p$ character, respectively. For the four silicon neighbors, they represent the total $3s+3p$ contributions on those atoms to the a_1 and t_2 components of each defect orbital.

The interaction between these two states is evident in the figure, the a_1 and t_2 character of the two orbitals tending to reverse with displacement. The transition is not abrupt, indicating significant off-diagonal coupling G . On the other hand, the fact that the two orbitals have comparable a_1 and t_2 character at the equilibrium displacement indicates that the levels have almost crossed ($IQ_0 \sim \Delta$). The origin of the nitrogen displacement therefore appears to be associated with the Jahn-Teller instability of the nearby unoccupied $4t_2$ state, i.e., a pseudo-Jahn-Teller effect.

These arguments are also confirmed in the experimental results. Brower⁵ found from ^{14}N hyperfine analysis that the wave function on the nitrogen was 72% p and 28% s , similarly reflecting the strong t_2 character on the central atom. The t_2 character of the ligands is also evidenced by strong hyperfine interaction with only the $\langle 111 \rangle$ silicon atom. Our a_1' state is computed to be localized $\sim 8\%$ on the nitrogen, $\sim 22\%$ on the $\langle 111 \rangle$ silicon, and $\sim 3\%$ on the remaining three silicons. The nitrogen charge and large ratio of $\text{Si}\langle 111 \rangle$ to Si_3 charge is therefore consistent with experiment. We note, however, that the EPR results indicate significantly more charge on the $\langle 111 \rangle$ silicon (72%) than we find (22%). This does not appear to be a small-cluster effect, since it persists even in the large-cluster (SI16) calculations. The description in terms of a pseudo-Jahn-Teller effect also explains the lack of displacement for C^0 or N^+ , because for these the $3a_1$ state is unoccupied.

These pseudo-Jahn-Teller arguments may be similarly presented in a many-electron (total-energy) framework. Here, the 2A_2 ground state is given by the configuration $\cdots (3a_1)^1(4t_2)^0$. The ground state in the lower symmetry is, therefore, primarily a linear combination of this state

and the A_1 partner in C_{3v} symmetry derived from the 2T_2 first excited state which has a configuration $\cdots (3a_1)^0(4t_2)^1$. It is the first excited state which appears to provide the driving force for the displacement.

We now consider the substitutional oxygen impurity. First, O^{2+} is found to remain on-center as C^0 and N^+ , while O^+ moves off center to a minimum in the $\langle \bar{1}\bar{1}\bar{1} \rangle$ direction as N^0 . Hence, the pseudo-Jahn-Teller arguments which we have used to describe the nitrogen systems, N^+ and N^0 , appear to apply to the isoelectronic impurities O^{2+} and O^+ , as well. The neutral-oxygen impurity, however, shown in Fig. 7, has only a saddle point in the $\langle \bar{1}\bar{1}\bar{1} \rangle$ direction, with a new deeper minimum in the $\langle 100 \rangle$ direction. This is also found to be true for O^- .

In Figs. 9(a) and 9(b) we show the a_1 and t_2 eigenvalue and wave-function character, respectively, for neutral oxygen as a function of $\langle 100 \rangle$ oxygen displacement. Here, the t_2 state splits into b_1 , a_1' (labeled a_1''), and b_2 states of C_{2v} . (A similar level structure is obtained for O^- , but with the extra electron in the b_1 state.) This is fully consistent with EPR studies of O^- which reveal the symmetry of the unpaired-electron orbital to be b_1 (Ref. 6). The b_1 state is found to be localized $\sim 0\%$ on the oxygen, $\sim 30\%$ on the two silicons opposite the oxygen $\langle 100 \rangle$ displacement, and $\sim 0\%$ on the remaining two silicons. This is consistent with experiment to the extent

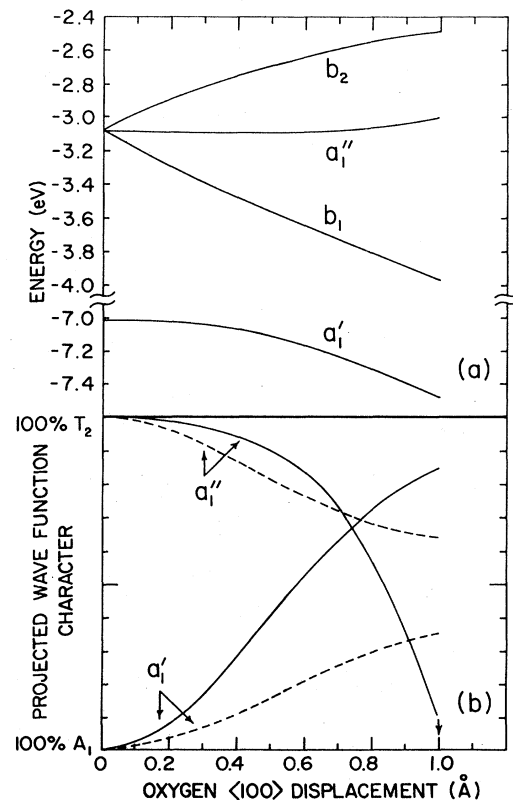


FIG. 9. (a) Energies of $3a_1$ (a_1') and $4t_2$ (b_1, a_1'', b_2) states vs oxygen $\langle 100 \rangle$ displacement for $\text{OSi}_4\text{H}_{12}$ ($d_{\text{Si-H}}=2.12 \text{ \AA}$) from MNDO. (b) Projected A_1 and T_2 (in T_d) character on oxygen (solid) and on ligands (dashed). The arrow on the displacement axis denotes the position of the minimum total energy.

that most of the ligand charge is on the silicons which are opposite the oxygen displacement. In absolute terms, however, this computed charge ($\sim 30\%$) again falls short of experiment ($\sim 70\%$), and, as with nitrogen, it does not appear to be a small-cluster effect.

Here again, the eigenvalues [Fig. 9(a)] and, particularly, the wave-function character [Fig. 9(b)] reveal interaction between the occupied a_1' and unoccupied a_1'' states. Therefore, the origin of the displacement again appears to be the Jahn-Teller instability and coupling of the nearby $4t_2$ state. In this case it would appear to be a pure pseudo-Jahn-Teller effect in the sense that no linear diagonal coupling for either of the two a_1 states can occur for a $\langle 100 \rangle$ central-atom displacement.

This two-level pseudo-Jahn-Teller model for oxygen may be expressed in a total-energy framework, as described earlier for nitrogen. Here we run into a problem, however, as the two-level linear-coupling model always predicts a deepest minimum in the trigonal ($\langle \bar{1}\bar{1}\bar{1} \rangle$) direction. This is not the case experimentally or from our calculation. That the oxygen $\langle 100 \rangle$ minimum is lower than the $\langle \bar{1}\bar{1}\bar{1} \rangle$ minimum suggests a partial breakdown of this simple model. Such a failure might be expected from a system which exhibits a large relaxation where quadratic terms and linear coupling to higher excited states may become important. The present manifestation of this appears to be a deepening of the $\langle 100 \rangle$ well relative to the $\langle \bar{1}\bar{1}\bar{1} \rangle$ well.

D. Cluster termination and size effects

We now consider the sensitivity of these predictions to variations in our cluster model of the impurity environment by (i) varying the Si-H distance in the SI4 clusters, and (ii) repeating these calculations using the SI16 clusters. We find that the off-center behavior is partially quenched for oxygen and fully quenched for nitrogen by either reducing the Si-H distance or by using the SI16 clusters. The abrupt nature of the nitrogen transition to the on-center position with reduced Si-H distance is clear from Fig. 10.

In order to understand why the degree of spontaneous displacement depends on the cluster in this way, we explore the SI4, SI4', and SI16 impurity environments by using a carbon atom as a probe. The carbon atom is well suited for this purpose, since it is a first-row atom such as nitrogen and oxygen, yet it has an on-center minimum in all cases. (As we have seen, this is a consequence of the a_1 gap state being unoccupied.) We consider first the SI4 and SI4' clusters. By monitoring the total energy as a function of carbon displacement from the on-center position, we find spring constants of 3.9 and 6.0 eV/Å² for carbon displacements in SI4 and SI4', respectively. This increase in the spring constant represents a stiffening of the lattice framework at the impurity site, which would tend to make it more difficult for an impurity to move off center in the SI4' cluster. Associated with this change in spring constant Δk is a change in the potential-energy surface of $\frac{1}{2} \Delta k Q^2$ for impurity displacement Q . Using the Δk of 2.1 eV/Å² predicted by our carbon-atom probe (6.0 - 3.9 eV/Å²), we find this additional energy sufficient

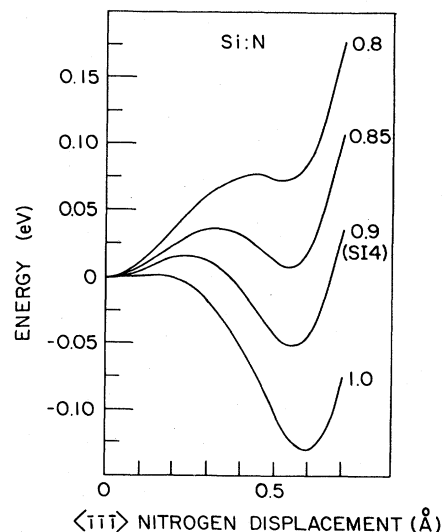


FIG. 10. Total energy of cluster $\text{NSi}_4\text{H}_{12}$ from MNDO as a function of nitrogen $\langle \bar{1}\bar{1}\bar{1} \rangle$ displacement for various Si-H distances. The numbers on the right-hand side of the figure (0.8, 0.85, 0.9, and 1.0) indicate the amount by which 2.35 Å is scaled to give the corresponding Si-H distance.

to quench the small nitrogen off-center minimum found with the SI4 cluster, but sufficient only to reduce the much larger oxygen off-center minimum. For example, the nitrogen minimum of -0.05 eV at 0.55 Å in the $\langle \bar{1}\bar{1}\bar{1} \rangle$ direction (SI4) would be raised in energy by 0.32 to $+0.27$ eV if we increase the spring constant as described. The SI4' energy at this displacement (from MNDO) is $+0.27$ eV, consistent with this model.

We can argue in a simple bond-orbital picture that this comes about because we have strengthened the Si-neighbor-to-Si-next-nearest-neighbor bonds. Viewed this way, the four Si bonds which point into the impurity region are now expected to be more sp^3 -like, as they would be for silicon atoms in crystalline silicon. Therefore, in the SI4' cluster, spontaneous impurity displacements would be less likely since the enhanced sp^3 character would favor a tetrahedrally coordinated impurity. Similar arguments apply to the quenching of impurity displacements in going from SI4 to SI16 as well. Since one might have expected this to be an improvement in the theory, especially in going to the SI16 clusters, it seems at first difficult to understand why the predicted nitrogen displacement is now incorrect. What this must mean is that our apparent success with the simple SI4 cluster is, at least in part, fortuitous.

E. Spontaneous impurity and near-neighbor displacements

The most obvious omission in our treatment of impurity relaxation so far is the failure to consider the response of the silicon atoms which form the environment of the impurity. In this section we explore the effect of including these additional relaxations by two separate simple models.

1. SI16 "rigid-cage" model

We consider first the spontaneous displacements of the four near-neighbor silicons in our SI16 cluster, with the impurities at the origin and all other atoms held fixed (the $\text{Si}_{12}\text{H}_{36}$ part of $\text{XSi}_{16}\text{H}_{36}$ now represents our rigid cage).

We begin with a fully symmetrical relaxation (a_1 symmetry) of these four silicon atoms. When a silicon atom is at the center of the SI16 cluster, the near neighbors are found to remain essentially at their perfect-crystal sites, as mentioned earlier. The near-neighbor silicons relax outward by ~ 0.1 Å when the central silicon is removed, creating a lattice vacancy. This direction is consistent with the results of surface studies^{46,47} and recent Green's-function calculations on the lattice vacancy in silicon.⁴⁸ When the central silicon is replaced by either on-center carbon, nitrogen, or oxygen, the near neighbors are found to relax inward by ~ 0.35 Å. An inward relaxation of ~ 0.1 Å is found for on-center sulfur. Here, we find a substantial difference between the oxygen and nitrogen systems (which do displace off center) and the sulfur system (which does not). The larger sulfur atom appears to prevent such a large radial collapse of the near neighbors. However, now, with this inward silicon relaxation present, both the nitrogen and oxygen impurities are found to remain on center. *The off-center behavior is fully quenched by even small inward silicon displacements.* Again using the carbon atom as a probe of the impurity environment, we find that the spring constant with respect to carbon-atom motion increases from 4.2 to 17.3 eV/Å² as we impose this inward silicon displacement, consistent with this further quenching of the impurity displacements.

It would be quite difficult with a direct measurement to determine experimentally if this predicted inward displacement of 0.35 Å is reasonable. What is known from experiment, however, is that carbon, which remains on center, exhibits an infrared absorption (local mode) with wavelength 16.5 μm (Ref. 3). Our spring constants of 4.2 and 17.3 eV/Å² correspond to carbon oscillations with wavelengths of 32.6 and 16.0 μm, respectively. It is clear, therefore, that at least for carbon, the inward silicon relaxation is necessary to obtain agreement with infrared measurements; only then is the predicted spring constant sufficiently large. Such an inward collapse is certainly not surprising for the case of a small first-row atom replacing silicon. This observation, however, does not solve the problem for nitrogen or oxygen, which are known from experiment to go off center.

It is also known from experiment that there is a substantial tetragonal component to the silicon displacement about the substitutional oxygen impurity.⁶ This means that the near-neighbor silicons pinch together in a pairwise manner, as they do in the neutral- and negative-charge states of the lattice vacancy.⁴⁹ Therefore, we have explored this symmetry-lowering e_θ displacement in the presence and absence of the a_1 displacement described above, again with oxygen on center. We find very large e_θ spring constants (~ 9 eV/Å²) for $Q_{a_1} = 0.35$ Å "in" and ~ 13 eV/Å² for $Q_{a_1} = 0$, where energies are given per atom for actual atom displacements) and no spontaneous

e_θ displacements in either case.

The source of the large- e_θ spring constant calculated above is readily found to be the substantial bond stretching which occurs between near- and next-nearest-neighbor silicon atoms. This is, of course, a consequence of our freezing the atoms outside of this first shell of silicons (i.e., our rigid cage). In reality, more distant silicon neighbors could respond to the near-neighbor silicon e_θ displacements by relaxing through bond-bending modes which have associated with them small spring constants, e.g., these are perhaps represented mainly by the soft silicon TA modes. Hence, in order to properly account for the total-energy change with respect to the e_θ displacement, it would be necessary to consider the recovery of many more distant shells of silicon atoms to the motion of the four near neighbors. The need for such a distant-neighbor recovery was recognized by Larkins and Stoneham,⁵⁰ and more recently by Baraff, Kane, and Schlüter⁵¹ in their treatment of the lattice vacancy in silicon where a modified Keating model was used to simulate this effect.

The exploratory calculations described above reveal practical difficulties associated with our SI16 rigid-cage model, where only near-neighbor silicon displacements are included. A softening of the SI16 lattice framework with respect to symmetry-lowering displacements appears to be necessary. In principle, this might be accomplished with a larger cluster by treating the response of more silicon atoms. Also, the inward collapse of the near neighbors which was found to quench the off-center behavior cannot be further explored without considering the coordinated motion of the impurity and neighbors. (Note that, thus far, we have considered only the motion of the impurity in a framework of undisplaced silicons, and vice versa.) In view of computer storage and time limitations, such an approach is not possible within the framework of our MNDO cluster model. We therefore consider a hybrid model which we describe in the following section.

2. Hybrid model

In this final set of calculations we consider the spontaneous displacements of the impurity and four neighboring silicon atoms simultaneously. Unlike our SI16 treatment, here we attempt to provide a more realistic framework in which the impurity and near-neighbor silicons can move. Ideally, one would like a large cluster where more-distant neighbor silicons respond properly to the displacements of these five atoms, unlike the rigid cage of the preceding section. In practice, however, because of the large number of coordinates we wish to vary, we must restrict this calculation to a very small cluster. Our hybrid model consists of two parts. First, we have an SI4' cluster where the hydrogen terminators are constrained to move with (i.e., they follow) the four silicon atoms. "Springs" are then connected to each of these silicon atoms to simulate the presence of more-distant silicon neighbors. Consider, for example, the springs on the $\langle 111 \rangle$ silicon. Since we are simulating the forces due only to silicon atoms outside of the near-neighbor shell, the springs for the $\langle 111 \rangle$ silicon are constructed to have a preferred $\langle 111 \rangle$ direction. They are, therefore, characterized by three quanti-

ties: (i) k_{\parallel} —the spring constant along the $\langle 111 \rangle$ direction, (ii) k_{\perp} —the spring constant perpendicular to the $\langle 111 \rangle$ direction (axial symmetry assumed), and (iii) the origin for the $\langle 111 \rangle$ spring, which is measured from the crystalline-silicon near-neighbor site, inward or outward along the $\langle 111 \rangle$ direction. The spring energy associated with the $\langle 111 \rangle$ silicon atom can be written as

$$E_{\text{spring}} = \frac{1}{2} k_{\parallel} (Q_{\parallel} - Q_{\parallel}^0)^2 + \frac{1}{2} k_{\perp} Q_{\perp}^2,$$

where Q_{\parallel} and Q_{\perp} are displacements from the crystalline-silicon site along and perpendicular to the $\langle 111 \rangle$ direction, respectively, and Q_{\parallel}^0 locates the $\langle 111 \rangle$ spring origin. With these added spring energies, the automatic minimization feature of the MNDO program is used to locate the total-energy minima. This is done separately for C_{2v} - and C_{3v} -symmetry displacements of the impurity and four silicon neighbors.

In this hybrid model our springs essentially describe the elastic properties of a lattice vacancy, in that they attempt to provide the forces on the four nearest-neighbor atoms surrounding a lattice site due to all of the lattice atoms except the central one. As a guide in the choice of the spring parameters, we consider two separate estimates for the lattice vacancy—a theoretical one based upon a valence-force treatment of the interatomic forces,⁵¹ and an experimental one based upon results for the lattice vacancy in diamond.^{52–55}

(a) *Valence-force estimate.* A large-cluster valence-force treatment of the lattice vacancy in silicon by Baraff, Kane, and Schlüter⁵¹ suggests force constants for the nearest-neighbor atoms of $k_{\parallel} = 1.87 \text{ eV}/\text{\AA}^2$ and $k_{\perp} = 3.7 \text{ eV}/\text{\AA}^2$ (simply the a_1 and e spring constants of Table V of Ref. 51 divided by 4), with the spring origins located at the near-neighbor crystalline-silicon sites. Using these values in our hybrid model, we find that nitrogen remains on center and oxygen displaces off center in the $\langle \bar{1}\bar{1}\bar{1} \rangle$ direction, inconsistent with experiment.

Physically, the most obvious source of error in such a valence-force treatment is the omission of important changes in the system's electronic structure associated with the removal or replacement of an atom. This is clearly seen in more rigorous treatments of the lattice vacancy, where the near-neighbor silicons are predicted to relax outward toward the triangle of next-nearest-neighbor silicons,⁴⁸ thus exhibiting a tendency to become sp^2 bonded with them. This effect would not be present in a valence-force treatment. In fact, in our hybrid model of the vacancy with valence-force-derived external springs, the silicon atoms are found to relax inward. This suggests that our spring origins ought to be located outward from the near-neighbor crystalline-silicon sites, properly reflecting the vacancy characteristic to back bond differently when the central silicon is not present.

We attempt to compensate for this deficiency by first using the valence-force-derived springs described above,⁵¹ but with origins for the $[111]$ springs displaced outward along the corresponding $[111]$ directions. We do this for displacements of 0.3, 0.6, and 0.9 Å. At 0.6 Å, everything remains qualitatively the same except for the emergence of a nitrogen minimum in the $\langle \bar{1}\bar{1}\bar{1} \rangle$ direction, but which is

still higher in energy than the minimum at the origin. At 0.9 Å, nitrogen displaces off center in the trigonal direction. Oxygen remains trigonal, but a tetragonal minimum begins to emerge. It appears, therefore, that with these spring constants, unreasonably large outward displacements of the spring origins would be necessary to obtain agreement with experiment. (A displacement of 0.78 Å brings a silicon atom to the plane of its three back-bonded neighbors). In fact, these and further exploratory calculations suggest that a large $k_{\parallel}:k_{\perp}$ ratio would also be required in order to achieve the observed $\langle 100 \rangle$ off-center impurity behavior for oxygen. A valence-force treatment, however, will always give a ratio k_{\parallel}/k_{\perp} which is less than 1. This is easily seen by considering an atom connected by springs, each characterized by k , to four fixed neighbors. The change in energy for motion in any direction is $k_{\text{eff}}Q^2/2$, where $k_{\text{eff}} = 4k/3$. If one spring is removed, thus creating a vacancy, we find $k_{\text{eff}} = 4k/3$ for motion perpendicular to the missing spring, but $k_{\text{eff}} = k/3$ for parallel motion; hence, this gives the ratio $k_{\parallel}/k_{\perp} = \frac{1}{4}$.

(b) *Experimental estimate.* The simple rigid-cage valence-force model above, with $k_{\parallel}/k_{\perp} = \frac{1}{4}$, predicts $k_e:k_{t_2}:k_{a_1} = 4:2:1$ for the E , T_2 , and A_1 vibrational modes for the vacancy, close to the results of the larger-cluster valence-force treatments.⁵¹ The corresponding phonon energies for the vacancy would be $\omega_e:\omega_{t_2}:\omega_{a_1} = 2:\sqrt{2}:1$. No direct experimental results exist for these values in the case of the silicon lattice vacancy. However, Davies⁵² has recently identified the characteristic e and t_2 side bands on the GR1 luminescence band associated with the neutral vacancy in the analogous material diamond. The phonons were found to be $\omega_e = 40 \text{ meV}$ and $\omega_{t_2} = 95 \text{ meV}$, corresponding to $k_{t_2}:k_e = 5.6:1$, the reverse of the valence-force prediction. Consistent also with this, an a_1 phonon of 80 meV observed on the ND1 band⁵³ currently believed to be associated with the negatively charged vacancy in diamond^{54,55} gives $k_{a_1} > k_e$.

This serves as direct experimental evidence that the simple valence-force treatment can be grossly in error. Specifically, it confirms that the equivalent k_{\parallel}/k_{\perp} spring ratio must be significantly larger than the valence-force estimate. To determine an alternative set of spring constants we therefore scale the values implied above for the diamond vacancy ($k_{a_1} = 18.5 \text{ eV}/\text{\AA}^2$ giving $\omega_{a_1} = 80 \text{ meV}$, $k_e = 4.6 \text{ eV}/\text{\AA}^2$ giving $\omega_e = 40 \text{ meV}$) to those appropriate for silicon. We can do this in two ways. (i) Multiply the diamond-vacancy frequencies by the ratio of silicon and diamond Raman frequencies. (ii) Multiply the diamond-vacancy spring constants by the ratio of silicon and diamond r_0/K values, where r_0 is the near-neighbor separation and K is the compressibility. The resulting a_1 and e silicon-vacancy spring constants are, respectively, 6.8 and $1.7 \text{ eV}/\text{\AA}^2$ by the Raman-frequency scaling, and 5.1 and $1.3 \text{ eV}/\text{\AA}^2$ by the r_0/K scaling. We now use the average of these two empirically inferred silicon-vacancy spring constants as a guide in determining our three adjustable parameters.

Our procedure is to take the spring origins at the crystalline-silicon sites and the progressively move them out. For each origin, we adjust our parallel and perpen-

dicular spring constants so that the a_1 - and e -vacancy spring constants match the experimentally inferred values. We use a short self-consistency cycle to achieve a relaxed conformation and spring constants appropriate to this conformation. For example, for spring origins displaced outward by 0.3 Å, parallel and perpendicular spring constants of 6.9 and 0.8 eV/Å², respectively, yield a relaxed vacancy conformation with near neighbors to the vacancy center relaxed outward by 0.23 Å and pinched together (tetragonal e_θ displacement) by 34.1°. These predictions appear fully consistent with the large tetragonal displacements found from experiment⁴⁹ and the outward breathing displacements found from other theoretical calculations⁴⁸ for the vacancy in silicon. The a_1 and e spring constants are found to be 5.8 and 1.6 eV/Å², respectively.

The need for an outward displacement of ~ 0.3 Å for this new parametrization is also evident in the calculations for the substitutional nitrogen and oxygen. Without an outward origin, we find that the observed nitrogen and oxygen off-center behavior is still quenched by the inward radial motion of the near-neighbor silicon atoms. As the spring origins are moved out, the spontaneous displacement sets in, but, if the outward displacement is significantly less than 0.3 Å, we find that the trigonal minimum for substitutional oxygen is deeper than the tetragonal minimum, contrary to experiment.⁶ In the results to be described below, we have therefore chosen the 0.3-Å outwardly displaced origin and the corresponding spring constants ($k_{\parallel} = 6.9$ eV/Å² and $k_{\perp} = 0.8$ eV/Å²).

We now explore the cluster total energy versus neutral substitutional nitrogen displacement, where now the four near-neighbor silicons respond to the motion of the impurity. The total energy as a function of nitrogen displacement is shown in Fig. 11. We find a minimum for a

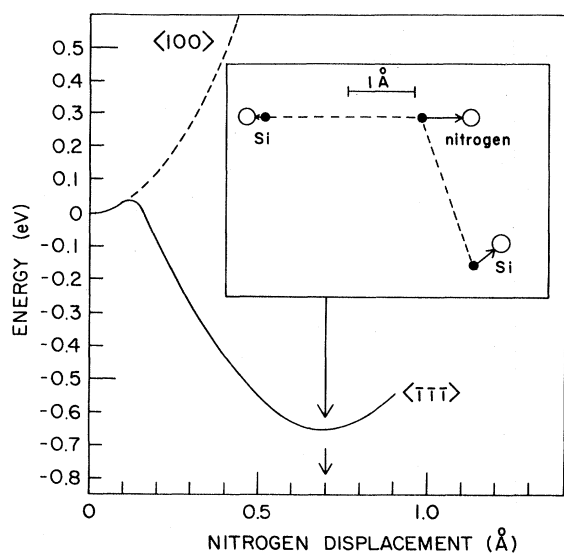


FIG. 11. Total energy of $\text{NSi}_4\text{H}_{12}$ cluster with external springs (hybrid model) from MNDO as a function of nitrogen displacement. Here, the silicon neighbors respond to the displacements of the impurity as described in the text. The inset shows the nitrogen and near-neighbor silicon positions at equilibrium in a (110) plane. Not shown are the other two near-neighbor silicons which are out of this plane.

nitrogen displacement of 0.70 Å in the $\langle \bar{1}\bar{1}\bar{1} \rangle$ direction, and a local minimum on center. This is in qualitative agreement with our SI4 cluster results. The response of the near-neighbor silicon atoms to the motion of the nitrogen as we move it off center is revealing. When nitrogen is fixed on center, the near-neighbor silicons relax inward by 0.27 Å. This is consistent with the SI16 calculation of the preceding section. As indicated earlier, an inward silicon relaxation of this magnitude would quench any off-center behavior. Up to a nitrogen displacement of ~ 0.1 Å, the silicons move in such a way as to preserve approximately the on-center tetrahedral coordination of nitrogen and silicons, i.e., the near neighbors are "dragged" along with the nitrogen. For larger $\langle \bar{1}\bar{1}\bar{1} \rangle$ nitrogen displacements, the $\langle 111 \rangle$ silicon springs back, exhibiting the outward relaxation characteristic of the lattice vacancy. The relaxed coordinates are shown in the inset of Fig. 11. Furthermore, the unpaired-electron charge is now 60% localized on the $\langle 111 \rangle$ silicon, in better agreement with the EPR studies of Brower.⁵ [We note, however, that a sizeable fraction of this increased localization over that of the SI4 cluster (22%) may be a consequence of moving in the hydrogen terminators, e.g., an SI4' calculation with an imposed nitrogen off-center displacement of 0.7 Å gives a localization of 51%.]

The important point here is that beyond a certain nitrogen displacement, the tendency of the silicons to collapse radially inward disappears and the previously described off-center characteristics prevail. The eigenvalues and eigenvectors have characteristics which are similar to those from the original SI4 calculations, so it again appears that a pseudo-Jahn-Teller mechanism operates.

Neutral oxygen is found to have a saddle point in the trigonal direction and a true minimum in the tetragonal direction, as shown in Fig. 12. This is again consistent with experiment⁶ and our earlier SI4 calculations. The near-neighbor silicons respond to the oxygen displacement in a manner which is similar to that of the nitrogen impurity. With oxygen fixed on center, the near-neighbor silicons move inward by 0.22 Å. This is again similar to the corresponding SI16 calculation. Beyond a critical oxygen displacement, the silicons which are opposite the oxygen $\langle 100 \rangle$ displacement direction spring back and pinch together, again exhibiting vacancylike characteristics. The final displacements are shown in the inset of Fig. 12. The localization of the first unoccupied state, which would accommodate the unpaired electron of O^- , is 62% on the silicons opposite the impurity direction. This again is in better agreement with the EPR studies,⁶ although much of this improvement again may be due to the moved-in hydrogen terminators. The pseudo-Jahn-Teller features are found to be similar to those of our earlier SI4 treatment.

The nature of the near-neighbor relaxations has been inferred by EPR studies⁶ and reveals primarily an e_θ displacement, consistent with the present results. Furthermore, infrared studies reveal that the ν_3 vibrational wavelength for oxygen is 12 μm (see Fig. 12 and corresponding caption).⁷ Our calculations give a value of 12.4 μm , in good agreement with experiment. Without the silicon displacements, the wavelength would be much too large, just as it was for substitutional carbon.

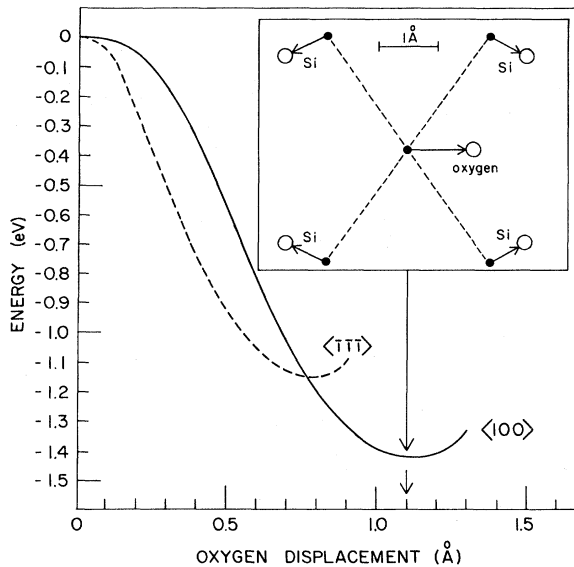


FIG. 12. Total energy of $\text{OSi}_4\text{H}_{12}$ cluster with external springs (hybrid model) as a function of oxygen displacement. Here, the silicon neighbors respond to the displacement of the impurity as described in the text. The inset shows the oxygen and near-neighbor silicon positions at equilibrium in the two perpendicular (110) planes (flattened into two dimensions on the figure for convenience). In this inset, the ν_3 vibrational mode would be represented by an "up-down" motion of the oxygen impurity.

Carbon and sulfur are found to be on center, consistent with experiment.²⁻⁴ The inward silicon relaxations for carbon and sulfur are 0.29 and 0.03 Å, respectively, consistent with the SI16 results. The carbon vibrational wavelength is 16.0 μm , again consistent with the SI16 calculation (16.0 μm) and experiment³ (16.5 μm). Also, negative oxygen is off center in a $\langle 100 \rangle$ direction, only now the silicons opposite the oxygen displacement direction are found to move apart. The angle between them increases from 76° to 101°, indicating the presence of a t_2 -symmetry displacement. These results are again fully consistent with experiment.⁶

Positive oxygen is found to go off center in the $\langle \bar{1}\bar{1}\bar{1} \rangle$ direction, consistent with our earlier SI4 calculations and pseudo-Jahn-Teller interpretation. Inconsistent with the previous SI4 calculation, however, is that O^{2+} is now found to displace even farther in this trigonal direction. This could be a small-cluster effect, associated with the large positive charge which builds up on the $\langle 111 \rangle$ silicon; that is, an anomalous electrostatic interaction similar to that called upon to explain off-center behaviors in ionic crystals. Large charge buildups of this kind are not reproduced in our SI16 calculations, suggesting that the O^{2+} displacement would not actually occur in the real crystal. We cannot, however, rule out the possibility that this is real effect, perhaps associated with the interactions of other occupied and unoccupied states which we have not considered, since this charge state of oxygen has never been observed. Positive nitrogen is found to remain on center, consistent with our SI4 treatment.

IV. DISCUSSION

The results of the hybrid model demonstrate that the quenching of the nitrogen and oxygen off-center behavior, as suggested by our SI16 calculations, can be averted if we (i) consider simultaneous impurity and near-neighbor relaxations, and (ii) provide a sufficient outward force on these silicons by a combination of large radial spring constants and outwardly displaced spring origins. The need for (ii), which is contrary to a simple valence-force treatment of the interatomic forces, suggests that a significant change in the near-neighbor-silicon back bonding occurs when the central silicon is either removed or replaced by an impurity. With these outward forces, the tendency for inward silicon-neighbor displacement still exists, but is sufficiently restrained (0.27 vs 0.35 Å for the SI16 cluster) to allow the off-center motion to take over. It is interesting to note that the final silicon near-neighbor positions (insets of Figs. 11 and 12) reveal relatively little and mostly outward radial displacements from their original positions, although the tendency for a "collapse" is still evident in that the nearest $\text{Si}_3\text{-N}$ and $\text{Si}_2\text{-O}$ distances are greatly reduced from the normal Si-Si distances. In effect, by partially restraining the uniform breathing-mode collapse of the silicon neighbors, the central atom is forced to go off center in order to nestle in closer to its silicon neighbors.

The question arises therefore as to whether the effective elastic properties of the near-neighbor silicon atoms implied by this hybrid model are realistic. In other words, are the displaced origins for the springs and the magnitudes of the spring constants (k_{\parallel} and k_{\perp}) deduced from the experimental estimate [Sec. III E 2(b)] reasonable? We consider these questions in order.

(1) We have argued earlier that an outward displacement of the spring origins is reasonable in the sense that we are considering the forces on the silicon neighbors in the *absence* of the central atom. It is well known that threefold-coordinated atoms in covalent molecules tend to go planar with sp^2 bonding. In the silicon lattice with the next-nearest shell fixed in position, the silicon near neighbors would be planar at 0.78 Å outward displacement. Clearly any reasonable fraction of this could be rationalized for the displaced origin.

(2) The magnitudes of the spring constants have been deduced by scaling directly from experimental values determined for the vacancy in diamond.⁵²⁻⁵⁵ This must be considered a strong argument that they are indeed realistic. They depart significantly, however, from the valence-force estimates (k_{\parallel} is significantly greater, k_{\perp} correspondingly less) for both silicon and diamond. Because the valence-force model is a simple and intuitively reasonable model, it is surprising that it could be so far off. Other evidence of its failure, however, also exists: Theoretical estimates for silicon and diamond^{50,56-59} and direct experimental measurements for silicon⁴⁹ both indicate large trigonal Jahn-Teller coupling coefficients for the vacancy. With the valence-force parameters, trigonal displacements would be predicted. Instead, the displacement is observed to be tetragonal, indicating again that the trigonal force constant must be greater than the tetragonal

one, contrary to the valence-force prediction, and reflecting the stiffer radial springs with $k_{||} > k_{\perp}$. Finally, our calculations themselves appear to require these elastic properties in order to reproduce the well-documented off-center displacements for these first-row impurities.

At this juncture, we can only point out this large discrepancy between the valence-force prediction and what appears to be the actual elastic environment of the XSi_4 cluster. This represents a fundamental and important problem and a challenge to theorists. What really is the correct elastic environment for a small cluster of atoms in the diamond-structure lattice? All modern electronic-structure calculations of defects are of clusters in the sense that no matter how elaborate the actual calculation extends over only a small finite number of atoms. To handle lattice relaxation, a hybrid lattice-continuum connection to the rest of the lattice will always be required. With the recent emergence of electronic-structure—calculation techniques with pseudopotentials that supply reliable total energies, these questions can perhaps begin to be addressed.

A good recent example of this hybrid approach is the work of Baraff, Kane, and Schlüter⁵¹ on the vacancy in silicon. By combining a calculation of the linear tetragonal Jahn-Teller coupling coefficient for moving the four nearest neighbors in a self-consistent electronic Green's-function treatment with springs on these atoms derived from a valence-force treatment, they predicted the Jahn-Teller displacements and resulting negative- U behavior with remarkable accuracy, as subsequently verified by experiment.⁶⁰ Was this agreement an accident? Our arguments here suggest that it may have been. If they had calculated the trigonal coefficients, it is quite likely that they would have predicted even larger trigonal displacements (as all previous calculations invariably have^{50,56–59}), negating their good agreement. This points up the importance of addressing this problem.

In the present hybrid-model calculations, the changes in the nitrogen and oxygen eigenvalues and wave-function characters are similar to those found in the $SI4$ treatment, which considered only impurity displacements. Therefore, the pseudo-Jahn-Teller arguments of Sec. III C appear to apply here as well, where the unoccupied and Jahn-Teller-split $4t_2$ state provides the driving force for spontaneous displacement through its interaction with the occupied $3a_1$ state.

It is instructive to note that these $3a_1$ and $4t_2$ states for substitutional nitrogen and oxygen are mostly on the neighbors and only weakly on the central atoms. They are therefore more "vacancylike" than "central-atom-like," and can be considered to be made up mostly from the a_1 and t_2 "dangling-bond" vacancy orbitals. In fact, experimentally, the electronic structure and electron-lattice coupling determined by EPR studies for O^- are very similar to those determined in the same way for the negative-charge state of the isolated vacancy (V^-), which also exhibits a spontaneous C_{2v} displacement.^{6,49}

Viewed this way, the instabilities for both the nitrogen and oxygen atoms can be considered to come from the characteristic Jahn-Teller instabilities of the vacancy. These small, strongly electronegative first-row atoms bond

relatively weakly to the neighboring silicon-vacancy orbitals, leaving them partially intact as the $3a_1$ and $4t_2$ levels in or near the gap, as in Fig. 3. For nitrogen, the instability sets in only weakly and therefore in the predicted $\langle \bar{1} \bar{1} \bar{1} \rangle$ direction. For the more compact electronegative oxygen atom, with an extra electron, the displacement sets in more strongly, flipping over into the characteristic C_{2v} V^- mode.

There is an intriguing difference, however, between the instabilities of the isolated vacancy and those of these first-row atoms. The instabilities of the vacancy appear to require partial occupancy of the t_2 orbitals, with a conventional Jahn-Teller effect. There is no evidence, for instance, of pseudo-Jahn-Teller displacement for V^{2+} which has an $(a_1)^2$ configuration similar to that for O^0 . Both oxygen and nitrogen, on the other hand, appear to be pseudo-Jahn-Teller systems relying heavily on the off-diagonal coupling between the a_1 - and t_2 -vacancy orbitals.

The presence of a small central atom therefore appears to have enhanced the pseudo-Jahn-Teller instability associated with the vacancy. Our results suggest that this may occur in two ways.

(1) The presence will reduce the a_1 - t_2 vacancy splitting Δ because of the greater interaction with the a_1 symmetry ligand orbitals. This is illustrated in Fig. 3 and is borne out in the $SW-X\alpha$ results, Fig. 1, where the $3a_1$ - $4t_2$ splitting is ~ 0.5 eV, compared to the corresponding results for the vacancy of ~ 1.4 eV.⁶¹

(2) The off-diagonal coupling can be enhanced by the presence of the impurity ion. In fact, this is precisely what our results are telling us. In the $SI4$ cluster, we are only moving the central-ion and large off-diagonal effects result. A simple physical argument for this is as follows: Off-diagonal coupling between the a_1 and t_2 states produces a net displacement of charge between the ligands. There is no obvious physical driving force for this in the case of the isolated vacancy. Motion of a central strongly electronegative (and hence partially charged) atom, however, clearly encourages this.

Finally, our hybrid model has demonstrated for the first time the delicate balance that exists between the natural tendency for inward collapse around a small first-row atom, stabilizing it on center, and the pseudo-Jahn-Teller tendency of the impurity to move off center, bonding in effect with only two (oxygen) or three (nitrogen) of its neighbors. This competition suggests some interesting consequences. For instance, in a region of a silicon crystal with sufficiently strong compressional stress, our results suggest that oxygen would go on center and, as sulfur, become a double donor. This provides a possible simple model for the "thermal donors"⁶² (known to be double donors⁶³) that are formed by oxygen aggregation at $\sim 450^\circ\text{C}$ in silicon. Oxygen is normally incorporated interstitially in silicon. In this configuration, it nestles between two bonding silicon atoms, pushing them apart and providing a compressional field around it. A small interstitial oxygen aggregate is therefore strongly compressional, and a substitutional oxygen in the core could be forced on center with respect to its four silicon neighbors. This provides a natural explanation for the fact that there are a large number of distinguishable but generically similar

donors (different number of oxygen atoms in the aggregate), yet there appears to be a threshold size (approximately four oxygen atoms) for formation. To our knowledge, this model has not been previously suggested.

V. SUMMARY

The single-particle electronic structures and atomic displacements of substitutional nitrogen and oxygen (and, to a lesser degree, carbon and sulfur) in silicon have been studied using a cluster representation. The on-center electronic structures were generated by both the SW- $X\alpha$ and MNDO methods for the cluster XSi_4H_{12} , and by MNDO for the larger cluster $XSi_{16}H_{36}$. The MNDO method was used to study impurity and near-neighbor displacements by monitoring the cluster total energy.

The primary on-center result predicted by both electronic-structure methods is that a localized a_1 single-particle state is the last occupied state for neutral substitutional nitrogen, oxygen, and sulfur. An unoccupied but also localized t_2 state is found above it. This ordering of a_1 and t_2 states is independent of cluster size and cluster termination, at least to the extent that we have explored it. This ordering is consistent with the results of other recent calculations.

Using the MNDO method in the small-cluster representation (XSi_4H_{12}) with silicons frozen at crystalline sites, the displacement directions are correctly predicted for neutral nitrogen ($\langle\bar{1}\bar{1}\bar{1}\rangle$), oxygen ($\langle 100 \rangle$), carbon and sulfur (on center), and for negative oxygen ($\langle 100 \rangle$). By monitoring the single-particle eigenvalues and eigenvectors, we have identified what appears to be a pseudo-Jahn-Teller effect which provides the driving force for the spontaneous displacements. The presence of the impurity atom seems to enhance the a_1 - t_2 coupling beyond that of the lattice vacancy, and therefore encourages the spontaneous asymmetric displacement even though the t_2 state is not occupied.

We have failed to reproduce these displacements with the larger cluster ($XSi_{16}H_{36}$), finding no nitrogen off-center displacement and a substantially reduced oxygen displacement. The oxygen displacement disappeared as well when a symmetric displacement (spontaneous and inward) of the near-neighbor silicon atoms was included. This result is misleading, however, since (i) the impurities were frozen at the origin while the silicon displacement was imposed, and (ii) the $Si_{12}H_{36}$ cage was frozen and could not respond to the motion of the near-neighbor silicons.

These failures led us to examine critically the motion of the near-neighbor silicons and the corresponding role played by the response of more-distant shells of silicon

neighbors. We used the small-cluster XSi_4H_{12} (with hydrogen terminators at the natural Si-H distance of 1.48 Å) which permitted us to consider *simultaneously* the spontaneous displacements of the impurity and its four near neighbors. The effect of the host outside of this small cluster was simulated by springs connected to the four silicon atoms of the cluster. We first tried spring parameters derived from the large-cluster valence-force treatment of Baraff, Kane, and Schlüter⁵¹ for the lattice vacancy in silicon. These failed to give the predicted nitrogen and oxygen relaxations. We linked this failure to two deficiencies inherent in any valence-force treatment. (i) The e -symmetry spring constant is predicted to be too large relative to the a_1 - and t_2 -symmetry spring constants as evidenced by recent optical studies of the lattice vacancy in the similar material diamond. (ii) The valence-force treatment fails to take account of changes in the near-neighbor back bonding associated with the creation of the vacancy. We, therefore, adjusted our external springs so that our force constants for the lattice vacancy in silicon agreed with those determined from experiment for the diamond vacancy, but scaled to silicon. Also, we moved the spring origins radially outward to account for the tendency of the near neighbors to back bond differently, now with sp^2 characteristics, when the central silicon is missing. With these new parameters, we predict vacancy and substitutional carbon, nitrogen, oxygen, and sulfur relaxations in agreement with experiment. Furthermore, our simple pseudo-Jahn-Teller model for the spontaneous impurity displacement seems to prevail even though the energy surface is now complicated by the presence of silicon displacements. This treatment which includes silicon displacements on an equal footing with the impurity displacements does, however, suffer from the necessity of using a less-sophisticated cluster representation.

Finally, we have demonstrated the delicate balance between a first-row impurity's tendency to go off-center and the tendency of near-neighbor silicons to collapse inward and quench the off-center behavior. We suggest the latter conformation, driven by the strain field of nearby interstitial oxygens, as a possible model for the thermal donors in silicon.

ACKNOWLEDGMENTS

The authors are grateful to the Lehigh University Computing Center for the generous amount of computer time and assistance which was made available. This research was supported by the U.S. Navy Office of Naval Research Electronics and Solid State Science Program Contract No. N00014-76-C-1097.

¹For a recent review of defects in semiconductors, see S. T. Pantelides, *Rev. Mod. Phys.* **50**, 797 (1978).

²R. C. Newman and J. Wakefield, *J. Phys. Chem. Solids* **19**, 230 (1961).

³R. C. Newman and J. B. Willis, *J. Phys. Chem. Solids* **26**, 373 (1965).

⁴G. W. Ludwig, *Phys. Rev.* **137**, A1520 (1965).

⁵K. L. Brower, *Phys. Rev. Lett.* **44**, 1627 (1980); *Phys. Rev. B* **26**, 6040 (1982).

⁶G. D. Watkins and J. W. Corbett, *Phys. Rev.* **121**, 1001 (1961).

⁷J. W. Corbett, G. D. Watkins, R. M. Chrenko, and R. S. McDonald, *Phys. Rev.* **121**, 1015 (1961).

⁸G. K. Wertheim, *Phys. Rev.* **105**, 1730 (1957); **110**, 1272 (1958).

- ⁹D. E. Hill, *Phys. Rev.* **114**, 1414 (1959).
- ¹⁰R. O. Carlson, R. N. Hall, and E. M. Pell, *J. Phys. Chem. Solids* **8**, 81 (1959).
- ¹¹J. A. D. Matthew, *Solid State Commun.* **3**, 365 (1965).
- ¹²M. J. L. Sangster and A. M. Stoneham, *Philos. Mag. B* **43**, 597 (1981); *Phys. Rev. B* **26**, 1028 (1982).
- ¹³U. Öpik and M. H. L. Pryce, *Proc. R. Soc. London Ser. A* **238**, 425 (1957).
- ¹⁴M. D. Glinchuk, M. F. Deigen, and A. A. Karmazin, *Fiz. Tverd Tela (Leningrad)* **15**, 2048 (1973) [*Sov. Phys. Solid State* **15**, 1365 (1974)].
- ¹⁵W. D. Wilson, R. D. Hatcher, G. J. Dienes, and R. Smoluchowski, *Phys. Rev.* **161**, 888 (1967).
- ¹⁶G. Bemski, G. Feher, and E. Gere, *Bull. Am. Phys. Soc.* **3**, 135 (1958).
- ¹⁷W. V. Smith, P. P. Sorokin, I. L. Gelles, and G. J. Lasker, *Phys. Rev.* **115**, 1546 (1959).
- ¹⁸R. P. Messmer and G. D. Watkins, *Phys. Rev. B* **7**, 2568 (1973).
- ¹⁹S. Brand and M. Jaros, *Solid State Commun.* **21**, 875 (1977).
- ²⁰M. Astier, N. Pottier, and J. C. Bourgoin, *Phys. Rev. B* **19**, 5265 (1979).
- ²¹A. Mainwood, *J. Phys. C* **12**, 2543 (1979).
- ²²J. A. Vergés, *J. Phys. C* **14**, 365 (1981).
- ²³A. Chatterjee and C. E. Jones, *Bull. Amer. Phys. Soc.* **21**, 90 (1976).
- ²⁴V. V. Sidarik and A. N. Zhevno, *Phys. Status Solidi B* **107**, K57 (1981).
- ²⁵G. B. Bachelet, G. B. Baraff, and M. Schlüter, *Phys. Rev. B* **24**, 4736 (1981).
- ²⁶H. P. Hjalmarson, P. Vogl, D. J. Wolford, and J. D. Dow, *Phys. Rev. Lett.* **44**, 810 (1980); P. Vogl, in *Festkörperprobleme (Advances in Solid State Physics)*, edited by J. Treusch (Vieweg, Braunschweig, 1981), Vol. XXI, p. 191.
- ²⁷M. J. Caldas, J. R. Leite, and A. Fazzio, *Phys. Status Solidi B* **98**, K109 (1980).
- ²⁸V. A. Singh, A. Zunger, and U. Lindefelt, *Phys. Rev. B* **27**, 1420 (1983); V. A. Singh, U. Lindefelt, and A. Zunger, *Phys. Rev. B* **27**, 4909 (1983).
- ²⁹R. Car and S. T. Pantelides, *Bull. Amer. Phys. Soc.* **28**, 288 (1983).
- ³⁰M. Lannoo, *Phys. Rev. B* **25**, 2987 (1982).
- ³¹G. D. Watkins, G. G. DeLeo, and W. B. Fowler, *Physica (Utrecht)* **116B**, 28 (1983).
- ³²K. H. Johnson and F. C. Smith, Jr., *Phys. Rev. B* **5**, 831 (1972). *X α* computer program written by F. C. Smith, Jr., and K. H. Johnson, Massachusetts Institute of Technology, Cambridge, MA.
- ³³K. Schwarz, *Phys. Rev. B* **5**, 2466 (1972).
- ³⁴J. C. Slater, *The Self-Consistent Field for Molecules and Solids* (McGraw-Hill, New York, 1974).
- ³⁵M. J. S. Dewar and W. Thiel, *J. Amer. Chem. Soc.* **99**, 4899 (1977); **99**, 4907 (1977); M. J. S. Dewar, M. L. McKee, and H. S. Rzepa, *ibid.* **100**, 3607 (1978); W. Thiel, *Quantum Chemistry Program Exchange* **11**, 379 (1979).
- ³⁶J. A. Pople and D. L. Beveridge, *Approximate Molecular Orbital Theory* (McGraw-Hill, New York, 1970).
- ³⁷M. J. S. Dewar, J. A. Hashmall, and C. G. Venier, *J. Amer. Chem. Soc.* **90**, 1953 (1968).
- ³⁸C. C. J. Roothaan, *Rev. Mod. Phys.* **32**, 179 (1960).
- ³⁹G. G. DeLeo, G. D. Watkins, and W. B. Folwer, *Phys. Rev. B* **23**, 1851 (1981); **25**, 4962 (1982); **25**, 4972 (1982).
- ⁴⁰E. Merzbacher, *Quantum Mechanics* (Wiley, New York, 1970), p. 538.
- ⁴¹B. G. Cartling, *J. Phys. C* **8**, 3171 (1975); **8**, 3183 (1975).
- ⁴²L. L. Rosier and C. T. Sah, *Solid-State Electron.* **14**, 41 (1971); *J. Appl. Phys.* **42**, 4000 (1971).
- ⁴³W. S. Verwoerd, *J. Comp. Chem.* **3**, 445 (1982).
- ⁴⁴J. Waser and L. Pauling, *J. Chem. Phys.* **18**, 747 (1950).
- ⁴⁵R. Meier and Tae-Kyu Ha, *Phys. Chem. Minerals* **6**, 37 (1980); C. A. Ernst, A. L. Allred, M. A. Ratner, M. D. Newton, G. V. Gibbs, J. W. Moskowitz, and S. Topiol, *Chem. Phys. Lett.* **81**, 424 (1981).
- ⁴⁶H. D. Shih, F. Jona, D. W. Jepsen, and P. M. Marcus, *Phys. Rev. Lett.* **37**, 1622 (1976).
- ⁴⁷A. Redondo, W. A. Goddard III, T. C. McGill, and G. T. Sur-ratt, *Solid State Commun.* **21**, 991 (1977); J. Ihm and M. L. Cohen, *Phys. Rev. B* **21**, 1527 (1980); **22**, 2135(E) (1980).
- ⁴⁸U. Lindefelt (unpublished). M. Scheffler *et al.* (unpublished).
- ⁴⁹G. D. Watkins, in *International Conference on Lattice Defects in Semiconductors, Freiburg, Germany, 1974* (IOP, London, 1975), p. 1.
- ⁵⁰F. P. Larkins and A. M. Stoneham, *J. Phys. C* **4**, 143 (1971); **4**, 154 (1971).
- ⁵¹G. A. Baraff, E. O. Kane, and M. Schlüter, *Phys. Rev. B* **21**, 5662 (1980).
- ⁵²G. Davies, *J. Phys. C* **15**, L149 (1982).
- ⁵³G. Davies, *J. Phys. C* **7**, 3797 (1974).
- ⁵⁴E. V. Sobolev and A. P. Eliseev, *J. Struct. Chem. (USSR)* **17**, 802 (1976).
- ⁵⁵G. Davies, *Nature* **269**, 498 (1977).
- ⁵⁶J. Friedel, M. Lannoo, and G. Leman, *Phys. Rev.* **164**, 1056 (1967).
- ⁵⁷F. P. Larkins, *J. Phys. Chem. Solids* **32**, 965 (1971).
- ⁵⁸C. A. Coulson and F. P. Larkins, *J. Phys. Chem. Solids* **32**, 2245 (1971).
- ⁵⁹F. P. Larkins, *J. Phys. Chem. Solids* **32**, 2123 (1971).
- ⁶⁰G. D. Watkins and J. R. Troxell, *Phys. Rev. Lett.* **44**, 593 (1980).
- ⁶¹L. A. Hemstreet, *Phys. Rev. B* **15**, 834 (1977).
- ⁶²J. R. Patel, *Semiconductor Silicon, 1981* (The Electrochemical Society, Pennington, N. J., 1981) p. 189.
- ⁶³D. Wruck and P. Gaworzewski, *Phys. Status Solidi A* **56**, 557 (1979).